Available online at www.sciencedirect.com

ScienceDirect

IFAC PapersOnline CONFERENCE PAPER ARCHIVE

IFAC PapersOnLine 52-24 (2019) 334–339

On the Positioning of Sensors with Simultaneous Bearing and Range Measurement in Wireless Sensor Networks

M. Khan * **M. W. Khan** ** **N. Salman** *** **A. H. Kemp** ****

* *University of Engineering and Technology Peshawar, Pakistan.*
** *Lincoln Centre of Autonomous Systems, University of Lincoln, UK.*
*** *School of Civil Engineering, University of Leeds, UK.*
**** *School of Electronic and Electrical Engineering, University of Leeds, UK.*

Abstract: Hybrid range and bearing based approach towards active localization of beacons will be widely celebrated in the near future, due to the protocols used for data transmission through targeted beam of radiation in 5G networks. This technique, which is one of the building blocks of 5G infrastructure does not only allow extremely high data rates but will also allow the estimation of direction of arrival/departure of the signal. Thus, in this paper a hybrid angle/range based approach towards positioning is under focus. A linear least squares approach will be applied to the unbiased version of hybrid direction of arrival-time of flight (DoA-ToF) measurement model. Thus, the unbiasing constant is first calculated followed by the theoretical mean squares expression calculation, to be utilized for selecting only those reference beacons that guarantee an improvement in the accuracy of the least squares approach. A critical distance expression is also derived that determines the relationship between the noise variance of angle and range estimates in terms of the distance between nodes. Furthermore, a weighted least squares solution is presented which exploits the noise covariance matrix of the hybrid measurement model. Finally, the weighted solution is bounded by the linear Cramér-Rao bound (LCRB) for the hybrid signal model.

Keywords: Localization, wireless sensor networks, estimation, optimization, time of flight, direction of arrival.

1. INTRODUCTION

The global positioning system (GPS) is considered as a panacea for positioning and tracking of objects. However, it suffers from severe limitations in terms of accuracy, specifically if used indoors. Though promising innovations and services are available that enables, even cellphone based GPS to attain centimeter level accuracy, these services are not available on demand and are expensive to avail, for example real time kinematics. Thus, in wireless sensor networks (WSN), active beacon based approach is the preferred choice for positioning. Localization in WSN is achieved either by utilizing the range between sensor nodes [Guvenc and Chong (2009)] or the angle of arrival [Schmidt (1986)] of the impinging signal. The underlying technology used for ranging depends upon the degree of accuracy required for the application. For example, in robot navigation systems, the location of a robot is primarily estimated through 2D/3D ranging lasers like Hokuyo/Velodyne [Kneip et al. (2009), Himmelsbach et al. (2008)]. As a result, extremely accurate localization can be achieved. On the other hand, location of sensors in WSN are obtained using radio frequencies either via the time of flight (ToF) [Rabbachin et al. (2006)] or received strength (RS) [Ouyang et al. (2010)]. Due to their accuracy, ranging techniques based on ToF are preferred over RS based distance estimation. Interested readers are referred to Pozyx positioning [PozyxLabs (2015)], an ultrawideband and Marvelmind indoor GPS system [MarvelmindRobotics (2017)], an ultrasonic based position systems that utilize radio frequency.

Irrespective of the technology used, the underlying algorithm used for localization plays an important role in the robustness, computational load and accuracy of localization. This work builds upon the contributions in [Khan et al. (2014b)], where an unbiased version of DoA-ToF measurement model, a linear least squares (LLS) and its weighted least squares (WLS) estimators were proposed. The full derivation of the unbiasing constant used in the model will be presented here. It will also be shown that in some scenarios using all available information from all the beacons, unconventionally, deteriorate the accuracy of localization. Thus an optimal reference node (RN-Node with known location) selection algorithm will be designed and evaluated via Monte Carlo simulation. Furthermore, the relationship between noise variance of angle and range estimates is presented that is dependent on the distance between RN and target node (TN-Node with unknown location). This result will be verified via a numerical example and simulation. Finally, the weighted solution obtained in [Khan et al. (2014b)] will be bounded by Linear Cramér-Rao bound (LCRB).

10.1016/j.ifacol.2019.12.432

Literature Review: Hybrid localization models are widely studied by the WSN community. Some of the widely used algorithm utilizing the hybrid measurement model are discussed here. In [Khan (2017)], a hybrid measurement model is approached in a distributed fashion by utilizing an unsupervised learning technique known as locally linear embedding. The resulting algorithm achieve the same accuracy as LLS but gives the freedom of distributed implementation to designers. A two step algorithm is presented in [Wang et al. (2013)], in which the authors convert the differential angle measurements into distance measurement in the second step with the help of range measurements obtained in the first step, to obtain a high accuracy estimate of the TN. A cooperative version of hybrid DoA-ToF signal models is proposed in [Khan et al. (2014a)], which outperforms its non-cooperative counterparts at the cost of computational load. [Horiba et al. (2013)] presents an iterative technique that utilizes both angle and range simultaneously to detect the non line of sight (NLOS) component of the signal. In [Lategahn et al. (2013)], the extended Kalman filter (EKF) is used with time difference of arrival (TDoA) and DoA for tracking of human subjects. A Hybrid DoA and RS based measurement model is approached in [Salman et al. (2014)] where a LSS and a weighted solution is obtained.

The rest of the paper is organized as follows: Unbiased measurement model, LLS and WLS estimators are reviewed in section 2. In section 3, the unbiasing constant is derived followed by the derivation of critical distance expression. In section 4 the optimal RN selection is produced. The Cramér-Rao lower bound is presented in section 5 which is followed by section 6 which concludes the paper.

2. SYSTEM MODEL

For future reference we define the following notations: $Tr(.)$ and $(.)^T$ represent the trace and transpose operators, respectively. $E_x(.)$ represents the expectation operation with respect to random variable x, $x!$ denotes the factorial of x. A vector of N ones and N zeros is notated by $\mathbf{1}_N$ and $\mathbf{0}_N$, respectively.

Assumptions: A two dimensional network is considered. The network is composed of N RNs with known locations and M TNs whose location is to be estimated. A fully connected network is under focus. Readers interested in partially connected networks with hybrid measurements are referred to [Khan (2017)]. The i^{th} RN has predetermined coordinates i.e., X_i and Y_i. The vectors $\mathbf{X}=[X_1, ..., X_N]^T$ and $\mathbf{Y}=[Y_1, ..., Y_N]^T$ denote the vectors of x and y coordinates of all RNs. While the TN's coordinates are given by the vector $\mathbf{u}=[x, y]^T$. Finally, it is assumed that all RNs are capable of hybrid range and direction of arrival estimation.

When both ToF and DoA information is available at i^{th} RN, then the location of TN is calculated using

$$\hat{x} = X_i + \hat{d}_i \cos\hat{\theta}_i \delta_i \qquad \hat{y} = Y_i + \hat{d}_i \sin\hat{\theta}_i \delta_i \tag{1}$$

where $\hat{d}_i$, $\hat{\theta}_i$ are the noisy distance and angle estimates and δ_i is the unbiasing constant associate with i^{th} RN. In matrix form and for N RNs, (1) can be written as $\mathbf{Au}=\hat{\mathbf{b}}$, where

$$\mathbf{A} = [\mathbf{1}_N, \mathbf{0}_N; \mathbf{0}_N, \mathbf{1}_N] \in \mathcal{R}^{2N\times 2} \qquad \mathbf{u} = [x, y]^T \in \mathcal{R}^{2\times 1} \tag{2}$$

$$\hat{\mathbf{b}} = \begin{bmatrix} \mathbf{X} + \hat{\mathbf{d}} \cos\hat{\boldsymbol{\theta}}\boldsymbol{\delta} \\ \mathbf{Y} + \hat{\mathbf{d}} \sin\hat{\boldsymbol{\theta}}\boldsymbol{\delta} \end{bmatrix} \in \mathcal{R}^{2N\times 1} \tag{3}$$

and $\hat{\mathbf{d}}=\left[\hat{d}_1, \hat{d}_2, ..., \hat{d}_N\right]^T$, $\hat{\boldsymbol{\theta}} = \left[\hat{\theta}_1, \hat{\theta}_2, ..., \hat{\theta}_N\right]^T$ and $\boldsymbol{\delta} = [\delta_1, \delta_2, ..., \delta_N]^T$.

Linear Least Squares and Weighted Least Squares Solution

The measurement model presented in (1-3) can be solved for $\mathbf{u}$ using LLS approach as [Yu (2007)]

$$\hat{\mathbf{u}} = \mathbf{A}^{\dagger}\hat{\mathbf{b}} \tag{4}$$

where $\mathbf{A}^{\dagger}$ is the Moore-Penrose pseudo-inverse of $\mathbf{A}$. Alternatively, if N is known, $\mathbf{u}$ can be estimated in a linear least squares sense as

$$\hat{\mathbf{u}} = \frac{\mathbf{A}^T\hat{\mathbf{b}}}{N}. \tag{5}$$

A more accurate weighted solution can be obtained, if the covariance matrix, $\mathbf{C}(\mathbf{u})$, for the measurements in (1-3) is calculated. The covariance matrix is shown in (6), where $\boldsymbol{C}_x$, $\boldsymbol{C}_y$ and $\boldsymbol{C}_{xy}$ are $N \times N$ diagonal matrices with diagonal entries given by (26-28), the derivation of which will not be reproduced here; interested reader are referred to [Khan et al. (2014b)] and the references within.

$$\mathbf{C}(\mathbf{u}) = \begin{bmatrix} \boldsymbol{C}_x & \boldsymbol{C}_{xy} \\ \boldsymbol{C}_{xy} & \boldsymbol{C}_y \end{bmatrix} \in \mathcal{R}^{2N\times 2N}. \tag{6}$$

The weighted least squares estimator can then be obtained by minimizing

$$\mathbf{u}_{\mathrm{W}} = \left(\hat{\mathbf{b}} - \mathbf{Au}\right)^T \mathbf{C}^{-1}(\mathbf{u}) \left(\hat{\mathbf{b}} - \mathbf{Au}\right) \tag{7}$$

where the global minimum is obtained iteratively or through the closed form expression in (8)

$$\mathbf{u}_{\mathrm{W}} = \left(\mathbf{A}^T\mathbf{C}^{-1}(\mathbf{u})\,\mathbf{A}\right)^{-1} \mathbf{A}^T\mathbf{C}^{-1}(\mathbf{u})\,\hat{\mathbf{b}}. \tag{8}$$

The covariance matrix depends upon the true values of range and angle estimates, which are not available. Thus, there estimated values are used to get an estimated covariance matrix, $\widehat{\mathbf{C}}(\mathbf{u})$.

3. THEORETICAL ANALYSIS OF DOA-TOF MEASUREMENT MODEL

This section presents the derivation of unbiasing constant δ and introduces the notion of critical distances in DoA-ToF measurement models.

3.1 Calculation of unbiasing constant

It is observed that without considering the unbiasing constant, the LLS solution obtained in section 2 can only produce biased estimates of $\mathbf{u}$. It is imperative to remove this bias from the model before calculating the LCRB of the estimator. For any LLS estimator $\mathbf{u}$, the bias is calculated as [Kay (1993)]

$$\Delta = E_{(.)}[\hat{\mathbf{u}}] - \mathbf{u} \tag{9}$$

where Δ is the bias in estimation, $(.)$ is the source of noise in the observed measurements. For DoA-ToF, this will be the noise in range and angle estimates. Consider the noisy distance and angle estimate in (1). Let $\hat{d}_i = d_i + n_i$ and $\hat{\theta}_i = \theta_i + m_i$, where n_i and m_i are zero mean Gaussian

random variables of variance σ_i^2 and α_i^2 i.e., $n_i \sim \mathcal{N}\left(0, \sigma_i^2\right)$ and $m_i \sim \mathcal{N}\left(0, \alpha_i^2\right)$, respectively. Putting (4) in (9)

$$\begin{aligned} \Delta &= E_{(\mathbf{n},\mathbf{m})}\left[\mathbf{A}^{\dagger}\hat{\mathbf{b}}\right] - \mathbf{A}^{\dagger}\mathbf{b} \\ &= \mathbf{A}^{\dagger}\left(E_{(\mathbf{n},\mathbf{m})}\left[\hat{\mathbf{b}}\right] - \mathbf{b}\right) \end{aligned} \tag{10}$$

where $\mathbf{n}$ and $\mathbf{m}$ are the distance noise vector and the angle noise vector and $\mathbf{b}$ is the noise free version of $\hat{\mathbf{b}}$. Then the i^{th} term of Δ i.e., Δ_i is calculated as

$$\begin{aligned} \Delta_i &= E_{(n_i,m_i)}\left[(d_i + n_i)\cos\left(\theta_i + m_i\right)\right] - \left[d_i \cos\theta_i\right] \\ &= d_i E_{m_i}\left[\cos\left(\theta_i + m_i\right)\right] + E_{n_i,m_i}\left[n_i \cos\left(\theta_i + m_i\right)\right] \\ &\qquad - d_i \cos\theta_i. \end{aligned} \tag{11}$$

As $E_{n_i}\left[n_i\right] = 0$, (11) reduces to

$$\begin{aligned} \Delta_i = d_i \left[\cos\theta_i E_{m_i}\left(\cos m_i\right) - \sin\theta_i E_{m_i}\left(\sin m_i\right)\right] \\ - d_i \cos\theta_i. \end{aligned} \tag{12}$$

Expanding $\cos m_i$ and $\sin m_i$ through Taylor series, the following equation is obtained

$$\begin{aligned} \Delta_i = d_i \cos\theta_i E_{m_i}\left(1 - \frac{m_i^2}{2!} + \frac{m_i^4}{4!} - \frac{m_i^6}{6!}...\right) - \sin\theta_i \\ E_{m_i}\left(m_i - \frac{m_i^3}{3!} + \frac{m_i^5}{5!} - \frac{m_i^7}{7!}...\right) - d_i \cos\theta_i. \end{aligned} \tag{13}$$

All odd moments of zero mean Gaussian random variable are zero. Thus, after taking expectation w.r.t m_i (13) reduces to

$$\begin{aligned} \Delta_i &= d_i \cos\theta_i \left(1 - \frac{\alpha_i^2}{2} + \frac{3\alpha_i^4}{24} - \frac{15\alpha_i^6}{720} + ...\right) - d_i \cos\theta_i \\ &= d_i \cos\theta_i \sum_{n=0}^{\infty} \frac{\left(-\frac{\alpha_i^2}{2}\right)^n}{n!} - d_i \cos\theta_i. \end{aligned} \tag{14}$$

The summation in (14) is the Taylor series expansion of $\delta_i' = e^{-0.5\alpha_i^2}$. Thus (14) can be written as

$$\Delta_i = d_i \cos\theta_i \delta_i' - d_i \cos\theta_i. \tag{15}$$

Clearly, (15) can not be further reduced due to δ_i'. In order to force Δ_i to zero, one must introduce $\delta_i = e^{0.5\alpha_i^2}$ in the measurements, that cancels the effect of δ_i'. Thus, (15) is reduced to

$$\begin{aligned} \Delta_i &= d_i \cos\theta_i \delta_i' \delta_i - d_i \cos\theta_i \\ \Delta_i &= 0. \end{aligned} \tag{16}$$

Equ. (16) proves that in order to produce unbiased estimates, the utilization of δ_i is imperative.

3.2 Calculation of critical distance

While using the LLS approach, the error in the estimated coordinates of TN depends upon the noise variance of angle estimates, α_i^2, the noise variance of range estimates, σ_i^2 and the distance between RN and TN, d. This dependence on the internode distance is due to the fact that the noise variance of angle estimates are distance dependent. Meaning that α_i^2 will produce a large errors in the TN's position estimate, if the distance between RN and TN is larger, and smaller error at shorter distances. Thus we introduce the notion of critical distance.

Definition: "*The critical distance is the distance between RN and TN at which the effect of the noise variance of angle estimate and range estimate, on the accuracy of LLS estimate is equal*". In this section, the critical distance, d_c, is calculated as a function of σ_i^2 and α_i^2, using the theoretical mean squares error (MSE) of LLS estimator. The theoretical MSE for LLS estimator is given by [Kay (1993); Khan et al. (2014b)]

$$\mathrm{MSE}\left(\mathbf{u}\right) = Tr\left(\mathbf{A}^{\dagger}\mathbf{C}\left(\mathbf{u}\right)\mathbf{A}^{\dagger^T}\right). \tag{17}$$

The covariance matrix in (17) depends on both noise variances and the distance between RN and TN, as shown in (26-28). Equ.(18) represents the covariance matrix that is only dependant upon the distance noise variance, which can be obtained by forcing α_i^2 to zero in (26-28)

$$\mathbf{C}_n\left(\mathbf{u}\right) = \begin{bmatrix} \sigma_n^2\cos^2\theta & \sigma_n^2\cos\theta\sin\theta \\ \sigma_n^2\cos\theta\sin\theta & \sigma_n^2\sin^2\theta \end{bmatrix}. \tag{18}$$

Similarly, n_i free covariance is obtained by forcing σ_i^2 equal to zero in (26-28) and then plugging it in (6).

$$\mathbf{C}_m\left(\mathbf{u}\right) = \begin{bmatrix} \frac{d_c^2}{2}\left(\delta^2 + \frac{\cos 2\theta}{\delta^2}\right) - d_c^2\cos^2\theta & d_c^2\cos\theta\sin\theta\left(\delta^2 - 1\right) \\ d_c^2\cos\theta\sin\theta\left(\delta^2 - 1\right) & \frac{d_c^2}{2}\left(\delta^2 - \frac{\cos 2\theta}{\delta^2}\right) - d_c^2\sin^2\theta \end{bmatrix}. \tag{19}$$

Putting (18) in (17) for $\mathrm{MSE}_n\left(\mathbf{u}\right)$ and putting (19) in (17) for $\mathrm{MSE}_m\left(\mathbf{u}\right)$, which at the critical distance will be equal. Thus, [1]

$$\begin{aligned} \mathrm{MSE}_n\left(\mathbf{u}\right) &= \mathrm{MSE}_m\left(\mathbf{u}\right) \\ Tr\left(\mathbf{A}^{\dagger}\mathbf{C}_n\left(\mathbf{u}\right)\mathbf{A}^{\dagger^T}\right) &= Tr\left(\mathbf{A}^{\dagger}\mathbf{C}_m\left(\mathbf{u}\right)\mathbf{A}^{\dagger^T}\right). \end{aligned} \tag{20}$$

Equ. (20) can be reduced to

$$d_c = \sqrt{\sigma_n^2/\left(\delta^2 - 1\right)}. \tag{21}$$

Numerical Example: We take $\sigma_i^2 = 7$ m^2 and $\alpha_i^2 = 0.07$ rad, then $\delta^2 = 1.0723$. Using these values in (21) we get

$$d_c = \sqrt{7/\left(1.0723 - 1\right)} = 9.8\,\mathrm{m}. \tag{22}$$

This result is verified via the Monte Carlo simulation obtained in Fig. 3. The critical distance can be used in resource constrained networks, where a decision on whether to use ToF or DoA can be based on the critical distance analysis. In general, for networks where the average distance between the nodes is shorter then the critical distance, The DoA system should be advised by the developer. While for average distance larger than the critical distance, the ToF should be preferred.

4. ON THE PERFORMANCE OF LLS AND WLS

This section introduces a RN selection based approach to improve the accuracy of LLS estimation. A lower bound is also derived for the WLS to show the best possible accuracy achievable with the estimator.

4.1 Best RNs Selection

Conventionally in the presence of more RNs, the accuracy of localization improves. However this is not always the case. Some RNs that are situated at larger distances from the

[1] We consider $N = 1$, thus $\mathbf{A}$ will be an identity matrix of size 2.

TN and/or receives signal after multiple reflection actually deteriorate the overall performance of the system. Hence an optimal subset of RNs can achieve better accuracy than using all RNs. Thus in this section an optimal RN selection algorithm is designed that guarantees the best performance in a linear least square sense. This optimal combination of RNs is based on the theoretical MSE of LLS estimator Let $\overline{\mathrm{RN}}$ be the set of N RNs i.e.,

$$\overline{\mathrm{RN}} = \{\mathrm{RN}_1, \mathrm{RN}_2, \cdots, \mathrm{RN}_N\}$$

and let C represent any combination of RNs, then $\mathrm{C} \subseteq \overline{\mathrm{RN}}$, where the total number of subsets is given by $2^N - 1$. The optimum combination $\mathrm{C}_{\mathrm{opt}}$ is the one that minimizes the MSE of localization, i.e.,

$$\mathrm{C}_{\mathrm{opt}} = \arg\min_{\mathrm{C}} \mathrm{MSE}(\mathbf{u}). \tag{23}$$

The MSE expression again depends on the actual distances and angles which are unknown. Hence their estimates are used in (17). Thus a small number of RNs (in some cases even one RN) can achieve superior performance than using all RNs.

4.2 Cramér-Rao Lower Bound

The Cramér-Rao lower bound characterizes the best possible accuracy that can be achieved by an unbiased estimator. The LCRB can be obtained from the Fisher information of the system. Let $\mathbf{I}$ be the 2×2 Fisher information matrix (FIM) for hybrid DoA-ToF measurement model, then the element at i^{th} row and j^{th} column of FIM is given by (24), the full derivation of which can be obtained in [Kay (1993)]

$$\mathbf{I}_{i,j} = \mathbf{b}'_k \mathbf{C}^{-1}(\mathbf{u})\, \mathbf{b}'_l + \mathbf{0.5} Tr\Big(\mathbf{C}^{-1}(\mathbf{u})\, \mathbf{C}'_k(\mathbf{u})\, \mathbf{C}^{-1}(\mathbf{u})\, \mathbf{C}'_l(\mathbf{u})\Big) \quad \text{where } k,\ l = x, y \text{ for } i, j = 1, 2 \tag{24}$$

where $\mathbf{b}'_k = \partial \mathbf{b}/\partial k$ and k=x, y for i=1,2. Similarly, $\mathbf{b}'_l = \partial \mathbf{b}/\partial l$ and l=x, y for j=1,2. Taking the derivative of $\mathbf{b}$ w.r.t x, y results in the following equations

$$\mathbf{b}'_x = [\mathbf{1}_N; \mathbf{0}_N] \in \mathcal{R}^{2N\times 1} \qquad \mathbf{b}'_y = [\mathbf{0}_N; \mathbf{1}_N] \in \mathcal{R}^{2N\times 1}.$$

Similarly, $\mathbf{C}'_x(\mathbf{u})$ and $\mathbf{C}'_y(\mathbf{u})$ are the derivatives of the covariance matrix $\mathbf{C}(\mathbf{u})$, w.r.t x and y, respectively, the diagonal elements of which are given by (30-35).

With the FIM at hand, the MSE for a two dimensional system can be bounded as

$$\mathrm{MSE}(\mathbf{u}) \geq \frac{Tr(\mathbf{I})}{\det(\mathbf{I})}. \tag{25}$$

5. SIMULATION RESULTS

A network of 4 RNs and 30 TNs spread across 300m×200m area is considered. Some TNs are intentionally placed outside the convex hull formed by the 4 RNs to represent a more generalized network. Subsets of RNs and TNs are considered for each simulation and all simulation are run independently ℓ number of times. The network deployment is shown in Fig. 1.

Fig. 2 demonstrates the performance comparison between LLS and WLS solution in terms of average root mean square error (Avg. RMSE). It is evident from the figure that WLS performance is considerably better than the LLS.

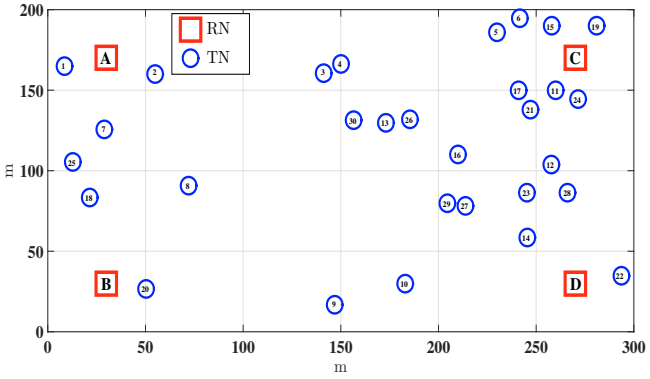

Fig. 1. Network deployment.

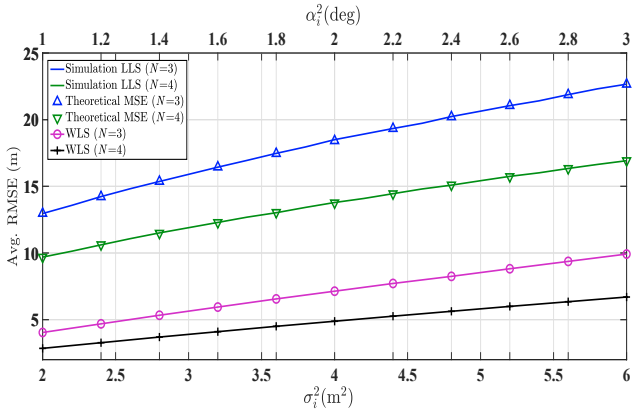

Fig. 2. Theoretical MSE and Performance comparison between LLS and WLS. RNs = [A, B, D] and [A, B, C, D], TNs = [1 − 30] , ℓ = 3000.

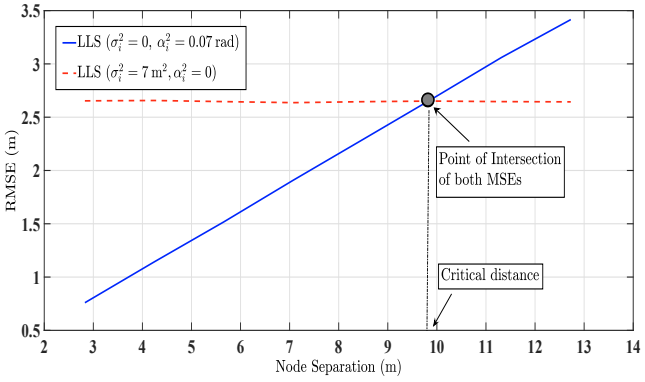

Fig. 3. Critical distance via Monte Carlo simulation, ℓ = 1000.

The figure also demonstrates the accurate prediction of LLS accuracy via the theoretical MSE expression.

The numerical example presented in section 3.2 to calculate the critical distance between a RN and a TN analytically, is verified via Monte Carlo simulation for 1000 Monte Carlo runs in Fig. 3. It is observed that for a fixed noise variance of range and bearing estimate, the critical distance calculated via (21) coincides with the critical distance obtained via simulation.

In Fig. 4 the performance is evaluated for different combinations of RNs. It is observed that the combination [A, C, D]

Covariance matrix for hybrid DoA-ToF measurements, [Khan et al. (2014b)].

$$\boldsymbol{C}_{x_i} = \left(\frac{d_i^2}{2} + \frac{\sigma_i^2}{2}\right) e^{\alpha_i^2} + \left(\frac{d_i^2}{2}\cos 2\theta_i + \frac{\sigma_i^2}{2}\cos 2\theta_i\right) e^{-\alpha_i^2} - (d_i \cos\theta_i)^2 \tag{26}$$

$$\boldsymbol{C}_{y_i} = \left(\frac{d_i^2}{2} + \frac{\sigma_i^2}{2}\right) e^{\alpha_i^2} - \left(\frac{d_i^2}{2}\cos 2\theta_i + \frac{\sigma_i^2}{2}\cos 2\theta_i\right) e^{-\alpha_i^2} - (d_i \sin\theta_i)^2 \tag{27}$$

$$\boldsymbol{C}_{xy_i} = \left(d_i^2 + \sigma_i^2\right)\cos\theta_i \sin\theta_i e^{-\alpha_i^2} - d_i^2 \cos\theta_i \sin\theta_i \tag{28}$$

$$\boldsymbol{C}_{x_{ij}} = \boldsymbol{C}_{y_{ij}} = \boldsymbol{C}_{xy_{ij}} = 0 \tag{29}$$

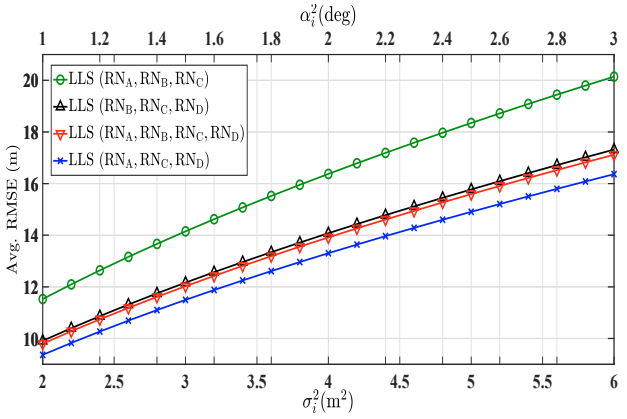

Fig. 4. Best RN selection. RNs=[(A,B,C), (B,C,D), (A,C,D), (A,B,C,D)], TNs=[5, 11, 16, 17, 21, 23, 24, 26], $\ell = 3000$.

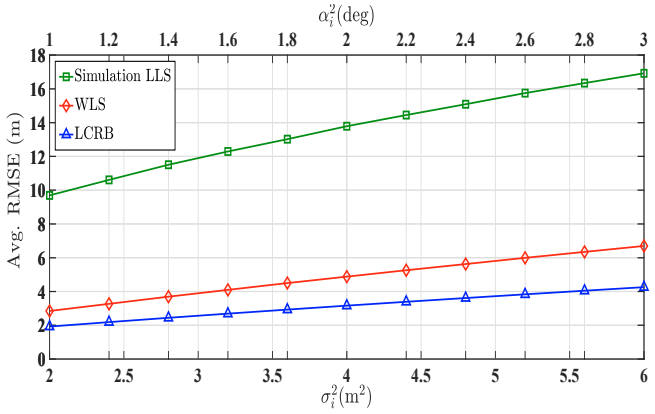

Fig. 5. LCRB comparison with WLS and LLS. RNs = [A − D] , TNs = [1 − 30], $\ell = 3000$.

gives a better accuracy than using all RNs simultaneously as shown by the combination [A, B, C, D]. For clarity purpose the performance of the rest of the combinations are not shown in the figure.

The LCRB is compared with WLS solution in Fig. 5. It is demonstrated that the LCRB presented in section 5 tightly bounds the performance of the WLS solution. For comparison the performance of LLS estimator is also presented.

6. CONCLUSION

An in-depth analysis of hybrid DoA-ToF measurement model for localization in WSN is presented in this work. It is observed that the classic hybrid measurement based LLS estimator for localization produces biased estimates of the unknowns. Thus an unbiased version of LLS and WLS estimators is produced and a unbiasing constant is derived. Also, based on the noise variance of angle and distance estimates, the notion of critical distance is introduced and an expression to calculate critical distance is derived. Furthermore, an optimal RN selection scheme is designed for LLS estimator to improve the performance of classic LLS approach for positioning. Finally, the WLS estimator is bounded by deriving the LCRB for the hybrid angle and range based measurement model.

REFERENCES

Guvenc, I. and Chong, C.C. (2009). A survey on ToA based wireless localization and NLOS mitigation techniques. *IEEE Communications Surveys Tutorials*, 11(3), 107–124.

Himmelsbach, M., Muller, A., Luettel, T., and Wuensche, H.J. (2008). LIDAR-based 3D object perception. In *Proc. of 1st International Workshop on Cognition for Technical Systems*.

Horiba, M., Okamoto, E., Shinohara, T., and Matsumura, K. (2013). An improved NLoS detection scheme for hybrid-ToA/AoA-based localization in indoor environments. In *IEEE International Conference on Ultra-Wideband (ICUWB)*, 37–42.

Kay, S.M. (1993). *Fundamentals of Statistical Signal Processing: Estimation Theory*. Upper Saddle River, NJ: Prentice Hall, Inc.

Khan, M.W. (2017). Relative positioning via iterative locally linear embedding: A distributed approach toward manifold learning technique. *IEEE Sensors Letters*, 1(6), 1–4.

Khan, M., Salman, N., and Kemp, A.H. (2014a). Cooperative positioning using angle of arrival and time of arrival. In *Sensor Signal Processing for Defence (SSPD)*, 1–5.

Khan, M., Salman, N., and Kemp, A.H. (2014b). Enhanced hybrid positioning in wireless networks I: AoA-ToA. In *IEEE International Conference on Telecommunications and Multimedia (TEMU)*, 86–91.

Kneip, L., Tache, F., Caprari, G., and Siegwart, R. (2009). Characterization of the compact hokuyo URG-04lx 2D laser range scanner. In *IEEE International Conference on Robotics and Automation*.

Lategahn, J., Muller, M., and Rohrig, C. (2013). TDoA and RSS based extended Kalman filter for indoor person localization. In *78th IEEE Vehicular Technology Conference (VTC Fall)*, 1–5.

MarvelmindRobotics (2017). Ultrasonic positioning system. `https://marvelmind.com/`.

Ouyang, R., Wong, A.S., and Lea, C.T. (2010). Received signal strength-based wireless localization via semidefinite programming: Noncooperative and cooperative schemes. *IEEE Transactions on Vehicular Technology*, 59(3), 1307–1318.

Derivative of covariance matrix for hybrid DoA-ToF measurements.

$$\frac{\partial}{\partial x}\boldsymbol{C}_{x_i} = \kappa_{x_i} e^{\alpha_i^2} + \sin 2\theta \kappa_{y_i} \left(1 + \cot 2\theta_i \kappa_{x_i} \kappa_{y_i}^{-1} + \sigma_i^2 d^{-2}\right) e^{-\alpha_i^2} - 2\kappa_{x_i} \tag{30}$$

$$\frac{\partial}{\partial y}\boldsymbol{C}_{x_i} = \kappa_{y_i} e^{\alpha_i^2} + \sin 2\theta \kappa_{x_i} \left(\cot 2\theta_i \kappa_{y_i} \kappa_{x_i}^{-1} - \sigma_i^2 d^{-2} - 1\right) e^{-\alpha_i^2} \tag{31}$$

$$\frac{\partial}{\partial x}\boldsymbol{C}_{y_i} = \kappa_{x_i} e^{\alpha_i^2} - \sin 2\theta_i \kappa_{y_i} \left(\cot 2\theta_i \kappa_{x_i} \kappa_{y_i}^{-1} - \sigma_i^2 d_i^{-2} - 1\right) e^{-\alpha_i^2} - 2\kappa_{y_i} \tag{32}$$

$$\frac{\partial}{\partial y}\boldsymbol{C}_{y_i} = \kappa_{y_i} e^{\alpha_i^2} - \sin 2\theta_i \kappa_{x_i} \left(1 + \cot 2\theta_i \kappa_{y_i} \kappa_{x_i}^{-1} - \sigma_i^2 d_i^{-2}\right) e^{-\alpha_i^2} \tag{33}$$

$$\frac{\partial}{\partial x}\boldsymbol{C}_{xy_i} = \kappa_{y_i} \left(2 \sin\theta_i \cos\theta_i \kappa_{x_i} \kappa_{y_i}^{-1} - \cos 2\theta\right) \left(e^{-\alpha_i^2} - 1\right) + \frac{\kappa_{y_i} \sigma_i^2 e^{-\alpha_i^2}}{d_i^2} \cos 2\theta_i \tag{34}$$

$$\frac{\partial}{\partial y}\boldsymbol{C}_{xy_i} = \kappa_{x_i} \left(2 \sin\theta_i \cos\theta_i \kappa_{y_i} \kappa_{x_i}^{-1} + \cos 2\theta\right) \left(e^{-\alpha_i^2} - 1\right) + \frac{\kappa_{x_i} \sigma_i^2 e^{-\alpha_i^2}}{d_i^2} \cos 2\theta_i \tag{35}$$

where $\kappa_{x_i} = (x - X_i)$ and $\kappa_{y_i} = (y - Y_i)$.

PozyxLabs (2015). Ultrawideband positioning system. `https://www.pozyx.io/`.

Rabbachin, A., Oppermann, I., and Denis, B. (2006). ML time-of-arrival estimation based on low complexity UWB energy detection. In *IEEE International Conference on Ultra-Wideband*, 599–604.

Salman, N., Khan, M.W., and Kemp, A.H. (2014). Enhanced hybrid positioning in wireless networks II: AoA-RSS. In *IEEE International Conference on Telecommunications and Multimedia (TEMU)*, 92–97.

Schmidt, R. (1986). Multiple emitter location and signal parameter estimation. *IEEE Transactions on Antennas and Propagation*, 34(3), 276–280.

Wang, Y., Wiemeler, M., Zheng, F., Xiong, W., and Kaiser, T. (2013). Two-step hybrid self-localization using unsynchronized low-complexity anchors. In *International Conference on Localization and GNSS (ICL-GNSS)*, 1–5.

Yu, K. (2007). 3-D localization error analysis in wireless networks. *IEEE Transactions on Wireless Communications*, 6(10), 3472–3481.